



Hydrographic changes in the Agulhas Recirculation Region during the late Quaternary

D. K. Naik¹, R. Saraswat¹, N. Khare², A. C. Pandey^{3,*}, and R. Nigam¹

¹Micropaleontology Laboratory, National Institute of Oceanography, Goa, India

²Ministry of Earth Sciences, New Delhi, India

³Allahabad University, Allahabad, India

*presently at: Bundelkhand University, Jhansi, India

Correspondence to: R. Saraswat (rsaraswat@nio.org)

Received: 14 August 2013 – Published in Clim. Past Discuss.: 30 September 2013

Revised: 11 February 2014 – Accepted: 2 March 2014 – Published: 15 April 2014

Abstract. The strength of Southern Hemisphere westerlies, as well as the positions of the subtropical front (STF), Agulhas Current (AC) and Agulhas Return Current (ARC) control the hydrography of the southwestern Indian Ocean. Although equatorward migration of the STF and reduction in Agulhas leakage were reported during the last glacial period, the fate of ARC during the last glacial–interglacial cycle is not clear. Therefore, in order to understand changes in the position and strength of ARC during the last glacial–interglacial cycle, here we reconstruct hydrographic changes in the southwestern Indian Ocean from temporal variation in planktic foraminiferal abundance, stable isotopic ratio ($\delta^{18}\text{O}$) and trace elemental ratio (Mg/Ca) of planktic foraminifera *Globigerina bulloides* in a core collected from the Agulhas Recirculation Region (ARR) in the southwestern Indian Ocean. Increased abundance of *G. bulloides* suggests that the productivity in the southwestern Indian Ocean increased during the last glacial period which confirms previous reports of high glacial productivity in the Southern Ocean. The increased productivity was likely driven by the intensified Southern Hemisphere westerlies supported by an equatorward migration of the subtropical front. Increase in relative abundance of *Neogloboquadrina incompta* suggests seasonally strong thermocline and enhanced advection of southern source water in the southwestern Indian Ocean as a result of strengthened ARC, right through MIS 4 to MIS 2, during the last glacial period. Therefore, it is inferred that over the last glacial–interglacial cycle, the hydrography of the southwestern Indian Ocean was driven by strengthened westerlies, ARC as well as a migrating subtropical front.

1 Introduction

The thermohaline circulation is responsible for distribution of heat across the world oceans. In the modern ocean, cold surface-ventilated water sinks to the bottom in the North Atlantic and around Antarctica, while the aged and gradually warmed water resurfaces in both the Indian and Pacific Ocean. The warmer water is transported back to the North Atlantic (Talley, 2013). The southwestern Indian Ocean is the conduit for transport of about 70 Sv of warm and salty water from the Indian Ocean into the Atlantic Ocean, via the eddy shedding by the Agulhas Current (AC) (Gordon, 1986; Bryden and Beal, 2001; Beal et al., 2011). A part of the AC retroflects off the southern tip of Africa and returns back to the Indian Ocean as the Agulhas Return Current (ARC) (Quartly and Srokosz, 1993; Lutjeharms and Ansoorge 2001; Quartly et al., 2006). The retroreflection depends on the inertia of the AC off Africa, wind stress over this region and the bottom topography (Lutjeharms and Ballegooyen, 1988; Le Bars et al., 2012). A distinct seasonality in the Agulhas Retroreflection (AR) is also observed with earlier retroreflection during austral summer than in winter (Matano et al., 1998). A few sporadic, large eastward shifts of the AR, leading to a disruption of eddy shedding and thus a reduction in the amount of water being transported from the South Indian to the South Atlantic Ocean, have also been observed (van Aken et al., 2013). A significant change in this inter-ocean water exchange has also been reported over the geologic period (Rau et al., 2002), especially the glacial terminations (Peeters et al., 2004; Barker et al., 2009). As the global thermohaline

circulation responds to the changes in the amount of water transported from the Indian and Pacific Ocean to the South Atlantic via the Agulhas Current in the southwestern Indian Ocean (Knorr and Lohmann, 2003; Beal et al., 2011), it is possible that the changes in the southwestern Indian Ocean may be a precursor to climate changes over the North Atlantic (de Ruijter et al., 2005; Marino et al., 2013). The strength of the ARC depends on the retroflexion as well as the position of the subtropical front (STF), which marks the transition between the tropical Indian Ocean and the Southern Ocean, and is distinguished as a sharp decrease in sea surface temperature (Rintoul et al., 2001; Anilkumar et al., 2006). The latitudinal migration of STF and processes associated with it affect transport of water from the southwestern Indian Ocean to the Atlantic Ocean by the Agulhas Current (Flores et al., 1999; Simon et al., 2013). As far as the link between westerlies and Agulhas leakage is concerned, contrasting views have been proposed. While paleostudies suggest reduced leakage associated with northward migration of westerlies and thus STF (Bard and Rickaby, 2009; Caley et al., 2012; Simon et al., 2013), the modeling studies suggest otherwise (Durgadoo et al., 2013). Even different paleostudies provide contrasting evidence and there is no consensus among the modeling studies either (Kohfeld et al., 2013). Further, the factors used to define the STF are also debated and it is suggested that bottom topography is also an important contributor in Agulhas leakage (De Boer et al., 2013; Graham and De Boer, 2013), necessitating more and more data from this region to understand Agulhas leakage dynamics. The response of ARC to the changes in the hydrography of the southwestern Indian Ocean over the glacial–interglacial timescales is not clear yet.

The physico-chemical state of the southwestern Indian Ocean is also an important component of the monsoon system and modulates the intensity and timing of the monsoon in India (Clemens et al., 1991), as well as in African regions (Bader and Latif, 2003). Any change in global climate will affect the thermal structure of the southwestern Indian Ocean, which in turn may act as feedback for further climate change. Therefore it is necessary to understand hydrographic changes in the southwestern Indian Ocean from the last glacial–interglacial transition, which will help to constrain the past climatic history of both the Indian monsoon as well the southeastern Atlantic Ocean. Limited information is available on past climatic history of the southwestern Indian Ocean. Foraminifera – single-celled, preferentially marine microorganisms with hard exoskeleton (test) – have ~ 30 extant species, each of which inhabits different depths of the water column. The foraminiferal tests accumulate on the seafloor, thus preserving the record of past water column structure. Therefore, here we have used changes in abundance, stable isotopic ratio ($\delta^{18}\text{O}$) and trace element ratio (Mg/Ca) of planktic foraminifer *Globigerina bulloides*, along with the relative abundance of *Neogloboquadrina incompta* (formerly *pachyderma* Dextral) (Darling et al., 2006)

to reconstruct paleoclimatic changes from the southwestern Indian Ocean, with an aim to understand changes in the strength of ARC over the last glacial–interglacial cycle.

Globigerina bulloides is abundant during periods of high phytoplankton productivity (Schiebel et al., 1997). It has a wide temperature tolerance limit and has been reported from almost all possible sea surface temperature ranges in the world oceans (Bé and Hutson, 1977; Hemleben et al., 1989; Sautter and Thunell, 1989). A several orders of magnitude higher abundance of *G. bulloides* is reported in the areas having a large phytoplankton population, as a result of upwelling nutrient-rich cold water from deeper depths to the surface (Peeters et al., 2002). Recently, Žarić et al. (2006) and Fraile et al. (2008) modeled the global distribution of planktic foraminiferal species, including *G. bulloides*, and found that this species is strongly correlated with highly productive regions. High-productivity regions are generally associated with upwelling induced by seasonal strong winds (Wyrki, 1971; McCreary et al., 1996). Thus the temporal variation in the relative abundance of *G. bulloides* in the Indian Ocean region has been suggested as an efficient tracer for the past changes in the surface productivity as a result of wind-driven upwelling associated with summer monsoon (Prell and Curry, 1981). A surface to near-surface habitat for *G. bulloides* in the southern Ocean was inferred based on $\delta^{18}\text{O}$ of the specimens collected in sediment traps (King and Howard, 2005). In view of reported increased abundance of *G. bulloides* in waters with high surface productivity, it has been widely used to infer paleo-upwelling and thus paleomonsoon changes in the Indian Ocean region (Gupta et al., 2003). *Neogloboquadrina incompta* prefers subsurface waters and its abundance is strongly correlated with high chlorophyll *a* concentration in pycnocline (Kuroyangi and Kawahata, 2004; Bergami et al., 2009). Increased relative abundance of *N. incompta* is also reported in upwelling areas including that around 40° S, though the effect of seawater temperature was also observed (Žarić et al., 2006; Fraile et al., 2008). Though the coiling direction ratio of *N. pachyderma* was proposed (Ericson, 1959) and frequently used as seawater temperature proxy, lately it was inferred that the differently coiled variants of *N. pachyderma* are in fact altogether different species, and further, that the right coiling morphospecies should be named as *N. incompta* (Darling et al., 2006).

The temperature-dependent replacement of Ca by Mg in both inorganically (Chave, 1954; Katz, 1973; Oomori et al., 1987) and organically precipitated carbonates (Lea et al., 1999; Rosenthal et al., 2000; Barker et al., 2005) lead to the application of Mg/Ca ratio of foraminiferal shells as seawater temperature proxy. The Mg/Ca ratio of *G. bulloides* is a reliable proxy of seawater temperature and has been frequently used to infer past hydrographic changes in the southwestern Indian Ocean (Martínez-Méndez et al., 2010; Simon et al., 2013). The Mg-Ca content of foraminiferal tests is, however, altered by post-depositional dissolution

(Brown and Elderfield, 1996) for which measures have been suggested for a few species to estimate temperature, after correcting for dissolution-induced changes (Rosenthal and Lohmann, 2002).

2 The study area

The study area lies in the southwestern part of the Indian Ocean, with the westward-flowing SEC as its northern boundary. The Madagascar bifurcates the westward-flowing SEC into the Mozambique Channel and the East Madagascar Current (EMC). The African subcontinent deflects the SEC, poleward. The poleward-deflected SEC, the Mozambique Channel and the East Madagascar Current (EMC) join together and flow further south as the Agulhas Current (Schott et al., 2009). The Agulhas Current frequently sheds rings as a result of retroflexion (Schouten et al., 2000). These rings carry warm and salty Indian Ocean water into the South Atlantic (de Ruijter et al., 1999). The Agulhas Current transports ~ 70 Sv of water, with contributions of 18 and 20 Sv from the Mozambique Channel and the East Madagascar Current, respectively (Donohue and Toole, 2003). A substantial part of the AC retroflects and flows as ARC, which joins the eastward-flowing Antarctic Circumpolar Current (ACC) and then completes the loop by flowing equatorward as the West Australian Current (Read and Pollard, 1993; de Ruijter et al., 2005). The core was collected from the ARR and falls in the path of ARC in the southwestern Indian Ocean which is characterized by a subtropical anticyclonic gyre (Stramma and Lutjeharms, 1997). The region around the core is marked by year-round strong upwelling due to interaction between EMC, Madagascar Ridge and local winds (Tomczak and Godfrey, 2003; Quartly et al., 2006; Poulton et al., 2009) as well as the factors associated with the Antarctic Circumpolar productivity belt (Ito et al., 2005).

The southwestern Indian Ocean receives surface waters from the subtropical gyre and subtropical current, which originate from the South Indian Ocean Current that flows north of the Circumpolar Current (Tomczak and Godfrey, 2003). Tritium data show that the Indonesian Throughflow contributes to a large part of the Indian Ocean surface water north of 40° S and down to the thermocline (Fine, 1985). The subtropical front (STF), located at $\sim 40^\circ$ S in the central South Indian Ocean, separates the warmer and saltier water of the subtropics from the cold, fresh, nutrient-rich subantarctic water (Stramma, 1992). The annual average sea surface temperature (SST) near the core location is 16.5°C while the salinity (SSS) is 35.3. The minimum (14.2°C) and maximum (18.9°C) SST at the core location is reported during austral winter and summer seasons, respectively. The SST during the other two seasons – i.e. spring (17.6°C) and fall (16.2°C) – differs by $\sim 1.5^\circ\text{C}$ (Locarnini et al., 2010). As compared to SST, small change (0.4 su) is observed in

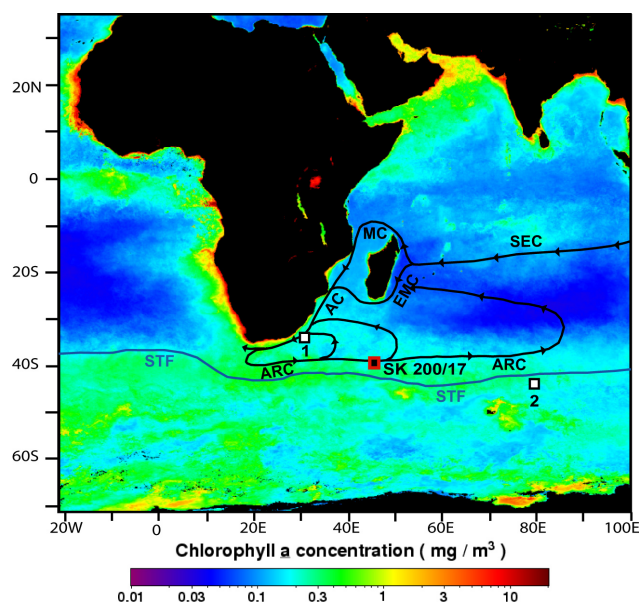


Fig. 1. The location of core SK 200/17 is marked with a red square. The surface circulation in this region, which includes the South Equatorial Current (SEC), Mozambique Channel (MC), East Madagascar Current (EMC), Agulhas Current (AC) and Agulhas Retroflexion/Return Current (ARC) is marked with black lines. The position of the subtropical front (STF) is marked with a thick dark blue line. The other cores discussed in the text are also marked as 1 (MD962077, Bard and Rickaby, 2009) and 2 (RC11-120, Mashiotta et al., 1999). The template is the average productivity in terms of chlorophyll *a* concentration in mg m^{-3} . The chlorophyll data was downloaded from the ocean color web page (<http://oceancolor.gsfc.nasa.gov/cgi/13>).

the surface seawater salinity, with the maximum SSS (35.4) reported during austral summer (Antonov et al., 2010).

3 Materials and methodology

The top 120 cm section of a gravity core (SK 200/17, hereafter referred to as SWIOC) collected from 39.03° S latitude and 44.97° E longitude, at a water depth of 4022 m was sampled every 1 cm (Fig. 1). The SWIOC was collected from the southwest Indian Ridge near the Indome Fracture Zone, at the northern boundary of modern high-productivity belt. The prominent topographic features surrounding this place include Agulhas Basin to the west, Mozambique Basin to the north west, Madagascar Basin to the northeast, Crozet Basin to the east and Crozet Ridge to the south. The core was collected as part of the “Pilot Expedition to the Southern Ocean” under the initiative of the National Centre for Antarctic and Ocean Research, Goa.

An appropriate amount (5–10 g) of sample was collected in pre-weighed and properly labeled petri dishes and oven dried at $45\text{--}60^\circ\text{C}$. The dried samples were weighed and

soaked in water for a minimum of 24 h. The overlying water was decanted after 24 h. The procedure was repeated several times until the overlying water became clear. The sediment sample was then washed by using a 63 μm sieve using a very slow shower so as to prevent foraminiferal test breakage. The fraction larger than 63 μm was then transferred in to small beakers for drying, then weighed and stored in plastic vials. The samples were dry-sieved using a 150 μm sieve and used for picking planktic foraminifera. An appropriate amount of > 150 μm sand fraction was taken after splitting. This representative fraction, so obtained, was weighed and uniformly spread over a gridded picking tray. From the representative fraction, all the planktic foraminiferal specimens were picked. From each sample, a minimum of ~ 300 specimens of planktic foraminifera were picked and mounted on micropaleontological slides. Out of the picked planktic foraminifera, all the specimens of *G. bulloides* were separated and counted by using “OLYMPUS SZX16” high-end research stereo microscope.

For stable oxygen isotopic analysis, 15–20 clean specimens of *G. bulloides* from 250–355 μm size range were picked. The specimens were gently crushed to break open all the chambers and washed three times with ultra-pure water, followed by methanol in 500 μL centrifuge tubes to remove clay and other extraneous material trapped inside the chambers. The cleaned fragments were transferred to glass vials for measurement in the mass spectrometer. The stable isotopic ($\delta^{18}\text{O}$) ratio was measured at the National Institute of Oceanography, Goa, India using “Thermo Finnigan isotope ratio mass spectrometer” calibrated via NBS 18 to the PDB scale. The values are given in δ -notation versus VPDB (Vienna Pee Dee Belemnite). The precision of oxygen isotope measurements, based on repeat analyses of NBS 18 and a laboratory standard, run over a long period was better than 0.1 ‰. For elemental (Mg/Ca) analysis, ~ 25 –30 clean specimens of *G. bulloides* from 250–355 μm size range were picked, weighed, crushed and transferred to plastic centrifuge tubes. The specimens were cleaned following the UCSB standard foraminifera cleaning procedure without the DTPA step (Martin and Lea, 2002). Thoroughly cleaned samples were analyzed by using a Thermo Finnigan Element2 sector field ICP-MS following the isotope dilution/internal standard method (Martin and Lea, 2002). The *G. bulloides* Mg/Ca ratio was converted to SST by using the calibration equation of Mashiotta et al. (1999).

$$\text{Mg/Ca} = 0.474(\text{exp } 0.107\text{Temp})$$

The error in Mg/Ca seawater temperature is $\pm 0.8^\circ\text{C}$, based on the error associated with the calibration equation. The planktic foraminiferal Mg/Ca ratio indicates the seawater temperature while $\delta^{18}\text{O}$ depends on both the seawater temperature and the oxygen isotopic ratio of the seawater. In order to assess the possible dissolution effect on foraminiferal Mg/Ca ratio, the shell weight was measured prior to crushing the tests for trace element analysis. The stable isotopic and

trace element data of SWIOC is compared with other cores (RC11-120) (Mashiotta et al., 1999), MD96-2077 (Bard and Rickaby, 2009), MD02-2594 and MD96-2080 (Martínez-Méndez et al., 2010) collected from the nearby region.

4 Chronology of the core

The $\delta^{18}\text{O}$ of *G. bulloides* from this core was compared with low latitude planktic foraminiferal global isostack (Bassinot et al., 1994) and cross-checked with $\delta^{18}\text{O}$ benthic foraminiferal global isostack of Lisiecki and Raymo (2005) to determine the tie points to establish the chronology (Fig. 2). A total of 7 tie points corresponding with Marine Isotopic Stage (MIS) 3, 4 and 5 and substage 2.2, 5.2, 5.4 and 5.5 were used to establish the chronology. The sedimentation rate varies from a minimum of 0.3 cm kyr^{-1} between 17–24 and 86–106 kyr to a maximum of 3.6 cm kyr^{-1} between ~ 9 and 17 kyr (average 1.1 cm kyr^{-1}). As only a few intact planktic foraminiferal shells were available in the core top sample, its age could not be determined. The next section with sufficient shells available for dating was 9–10 cm, which was radiocarbon dated to be 8600 ± 300 yr old. The dating was carried out at the Accelerator Mass Spectrometer facility of the Institute of Physics, Bhubneshwar, India. The chronology of the top 10 cm section was interpolated based on the sedimentation rate between 9 and 10 cm section and the age of MIS 2.2, taken as 17 kyr.

5 Results

The analyzed section covers a time span of 150 kyr at an average sample resolution of ~ 1 kyr. The core top is 7 kyr old, suggesting a loss of several top centimeters of the sediments during coring. The fraction > 63 μm was relatively more abundant during the early part of MIS 6 covered by the studied section and decreased to its lowest reported value throughout the core towards the MIS 6/5 transition (Fig. 3). The fraction > 63 μm almost entirely consists of planktic foraminiferal tests and its fragments. A gradual increase in planktic foraminiferal abundance, *G. bulloides* relative abundance and fraction > 63 μm is noted during MIS 5. The $\delta^{18}\text{O}$ *G. bulloides*, however, initially gets depleted from the bottom of the section until MIS 5.5 and subsequently becomes heavier until the MIS 5/4 transition. The *G. bulloides* relative abundance increases abruptly from the early MIS 4 to late MIS 4. A distinct enrichment of $\delta^{18}\text{O}$ *G. bulloides* is noticed during MIS 4. The *N. incompta* relative abundance remains unchanged throughout the MIS 4 only to increase abruptly towards MIS 4/3 transition. Decrease in Mg/Ca-based seawater temperature is also observed during the late MIS 4 (Fig. 3).

The planktic foraminiferal abundance and fraction > 63 μm increase from ~ 40 kyr onwards until the MIS 3/2 transition. The *G. bulloides* relative abundance

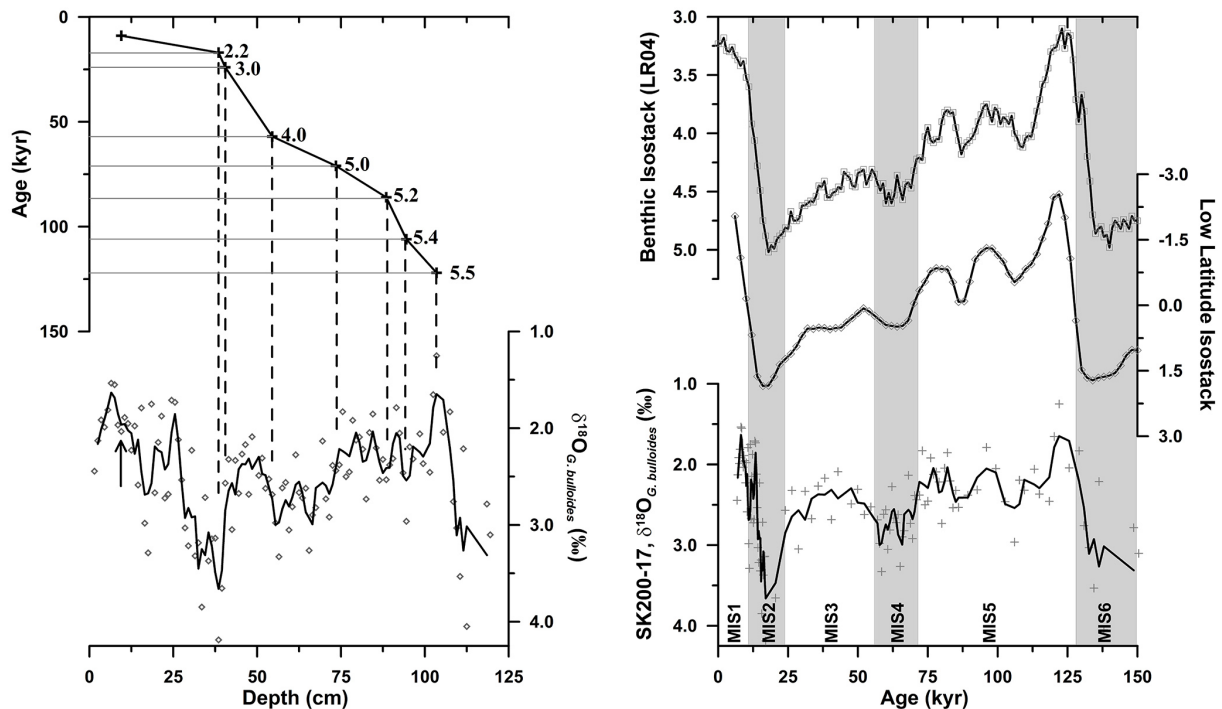


Fig. 2. The chronology of the core, as established by comparing the $\delta^{18}\text{O}$ *Globigerina bulloides* in the core with low latitude isostack map of Bassinot et al. (1994). This isostack curve was chosen as it is based on planktic foraminifera. The solid line represents three-point running average. The tie point isotopic events are marked by dashed and light lines as well as the numbers. The single AMS date at 9–10 cm depth interval is marked by an arrow. The final chronology of core SK 200/17 is compared with both the low-latitude isostack of Bassinot et al. (1994), as well as the benthic foraminiferal isostack (LR04) of Lisiecki and Raymo (2005).

decreases throughout the MIS 3 to reach a level towards the MIS 3/2 transition that is comparable with early MIS 5. The $\delta^{18}\text{O}$ *G. bulloides*, however, gets enriched from 40 kyr to the Last Glacial Maximum (LGM) corresponding to 17 kyr. The *N. incompta* relative abundance decreases during this interval, only to increase from ~35 kyr BP until the MIS 3/2 transition. The highest planktic foraminiferal abundance and fraction > 63 μm are noted during MIS 3/2 transition, whereas the *G. bulloides* relative abundance is at its lowest during this period.

During MIS 2, both planktic foraminiferal abundance and fraction > 63 μm decrease abruptly, whereas Mg/Ca seawater temperature and *G. bulloides* relative abundance increase. The $\delta^{18}\text{O}$ *G. bulloides* gets further depleted during the early part of MIS 2. The highest *N. incompta* relative abundance, however, is noted during late MIS 2. The Mg/Ca seawater temperature also increases from 20 kyr onwards until the MIS 2/1 transition. The planktic foraminiferal abundance, fraction > 63 μm and Mg/Ca seawater temperature increase during the early Holocene, whereas the *G. bulloides* relative abundance and *N. incompta* relative abundance decrease during the early Holocene. The $\delta^{18}\text{O}$ *G. bulloides* gets further depleted during the early Holocene. A decrease in *G. bulloides* shell weight is observed during the MIS 5. The shell weight increases from late MIS 5 and throughout MIS 4 until

early MIS 3. The shell weight decreases during early MIS 2 followed by an increase until the MIS 2/1 transition. A decrease in shell weight is observed during the early Holocene.

The LGM (taken as the average of five most depleted intervals centered at 17 kyr) early Holocene difference in $\delta^{18}\text{O}$ *G. bulloides* is $\sim 1.45 \pm 0.6\text{‰}$. The core-top Mg/Ca SST is 8.8 °C ($1.21\text{ mmol mol}^{-1}$ Mg/Ca), much lower than the average austral spring SST ($\sim 14.5\text{ °C}$) in the area. The LGM–Holocene difference in Mg/Ca seawater temperature is $1.2 \pm 1.2\text{ °C}$. The lowest Mg/Ca seawater temperature (6.5 °C at 21.2 kyr BP), however is $\sim 3\text{ °C}$ cooler than the average early Holocene Mg/Ca SST ($9.5 \pm 0.8\text{ °C}$). This lowest LGM Mg/Ca seawater temperature, however, is $\sim 8\text{ °C}$ lower than the average spring SST near the core site.

6 Discussion

6.1 Reliability of faunal data: comparison with previous work

Several post-depositional processes like slumping/turbidity currents, lateral transport, and dissolution affect foraminifera accumulated in the marine sediments, thus altering the original assemblage as well as the composition. Therefore, in order to assess the reliability of the faunal assemblages,

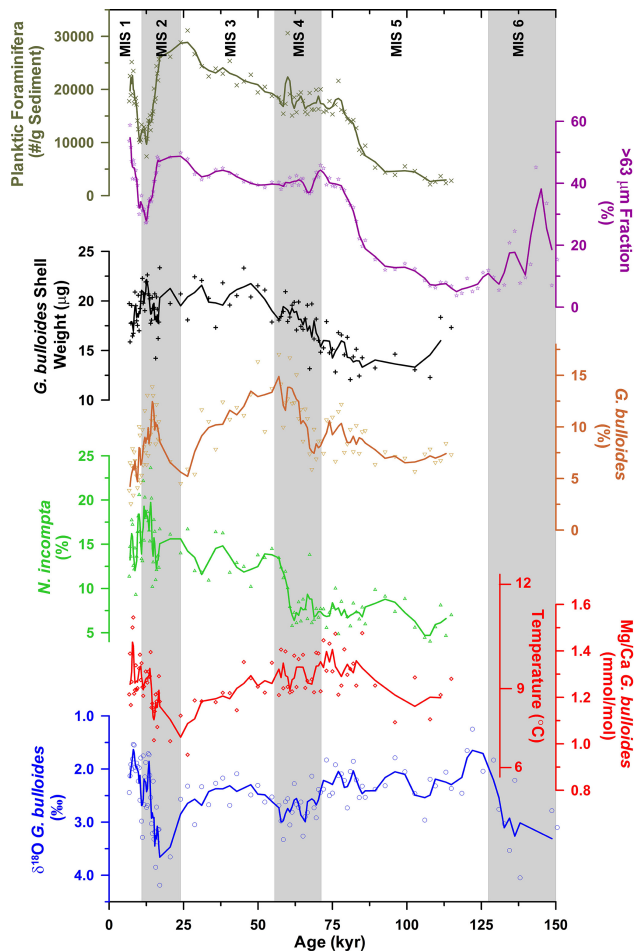


Fig. 3. Down-core variation in size fraction $> 63 \mu\text{m}$, planktic foraminiferal abundance (TPF/g sediment), average *Globigerina bulloides* shell weight, relative abundance of *G. bulloides* and *Neogloboquadrina incompta*, *G. bulloides* Mg/Ca along with estimated seawater temperature and $\delta^{18}\text{O}$. The symbols are the actual values, while the solid line is the three-point running average.

elemental and stable isotopic ratio in SWIOC, the core top data are compared with the previous studies, including water column, surface sediments as well as core tops from the nearby regions.

The average *G. bulloides* relative abundance during the early Holocene, in SWIOC ($6 \pm 2\%$), is lower than that in the plankton tow ($10.0\text{--}19.9\%$) and surface sediment samples ($20.0\text{--}49.9\%$) reported previously from the southwestern Indian Ocean (Bé and Hutson, 1977; Fraile et al., 2009). The abundance of *G. bulloides* is also lower than that at a southwesterly site where it comprises 20–30% of the planktic foraminiferal population in the sediments, whereas in the sediment traps, it constitutes up to 19–24% of the total planktic foraminifera, next only to *N. incompta* (King and Howard, 2003). The difference probably reflects the high spatial variability in the relative abundance of *G. bulloides* in this region as evident from very closely spaced *G. bulloides*

abundance contours around the core site (Bé and Hutson, 1977; Fraile et al., 2009). The average *N. incompta* relative abundance in the Holocene section of our core ($15 \pm 3\%$), however, is higher than its relative abundance in the plankton tows ($0.1\text{--}4.9\%$), but lower than that in the surface sediments ($20.0\text{--}49.9\%$) reported previously from this region (Bé and Hutson, 1977; Fraile et al., 2009). The difference in *N. incompta* abundance in the Holocene section of our core as compared to its relative abundance in the plankton tows probably reflects the seasonality associated with the plankton tows. A relatively higher abundance of *N. incompta* in a season other than the time when the plankton tows were collected will result in its higher relative abundance in surface sediments, as the surface sediments contain the foraminiferal assemblage accumulated over a long time period as compared to the snapshot seasonal nature of plankton tows.

The dissolution of foraminiferal tests can also cause difference in species abundance between sediments and plankton tows/sediment traps. As the susceptibility of foraminiferal species to dissolution is different, the dissolution is also likely to produce the difference in preservation between *G. bulloides* and *N. incompta*. Berger (1975) placed *G. bulloides* amongst one of the most dissolution-susceptible species, suggesting preferential dissolution of *G. bulloides* as compared to *N. incompta*. The modern carbonate saturation horizon in all three sectors of the Southern Ocean lies at $\sim 3400\text{ m}$ water depth (Howard and Prell, 1994). Increased carbonate dissolution during glacial periods is also reported from the Indian sector of the Southern Ocean. The cores recovered from the Cape Basin reveal that the carbonate saturation horizon during MIS 2 and 4 was $\sim 600\text{ m}$ shallower than present (Howard and Prell, 1994). The shallower carbonate dissolution horizon during MIS 2 and 4, may cause increased dissolution during these intervals. However, both the planktic foraminiferal number as well as the fraction $> 63 \mu\text{m}$ during MIS 4 are higher than that during MIS 5 and same as that during MIS 3 as well as MIS 1, suggesting otherwise. An abrupt decrease in both the planktic foraminiferal number as well as the fraction $> 63 \mu\text{m}$ is obvious during the MIS 2/1 transition, which clearly suggests poor preservation. The abrupt drop in *G. bulloides* relative abundance during early MIS 2 is, however, synchronous with the peak in planktic foraminiferal numbers as well as the fraction $> 63 \mu\text{m}$. The subsequent peak in *G. bulloides* relative abundance also coincides with poor carbonate preservation as inferred from decreasing planktic foraminiferal numbers, as well as the fraction $> 63 \mu\text{m}$. The anti-correlation between *G. bulloides* relative abundance and planktic foraminiferal numbers, as well as the fraction $> 63 \mu\text{m}$, suggests that carbonate preservation might not have significantly altered the planktic foraminiferal relative abundance at this location. As the core site already lies below the carbonate saturation horizon, any subsequent shallowing of the carbonate saturation horizon during a glacial period may not produce a large change in differential preservation of planktic foraminiferal species.

The possible differential diagenetic alteration of planktic foraminiferal assemblages, during glacial–interglacial period cannot, however be completely ruled out.

The early Holocene average $\delta^{18}\text{O}$ *G. bulloides* in our core ($2.1 \pm 0.4\text{‰}$) is same as that in RC11-120 ($2.2 \pm 0.3\text{‰}$) collected from comparable latitudes in the southeastern Indian Ocean. The average LGM $\delta^{18}\text{O}$ *G. bulloides* in our core ($3.5 \pm 0.5\text{‰}$) also matches with that in RC11-120 ($3.4 \pm 0.1\text{‰}$) (Mashiotta et al., 1999). The early Holocene average Mg/Ca *G. bulloides* in our core ($1.31 \pm 0.11 \text{ mmol mol}^{-1}$) is lower than that in RC11-120 ($1.60 \pm 0.07 \text{ mmol mol}^{-1}$). The LGM average Mg/Ca in our core ($1.16 \pm 0.11 \text{ } \mu\text{mol mol}^{-1}$) is, however, comparable with that in RC11-120 ($1.10 \pm 0.07\text{‰}$). The lower average Holocene Mg/Ca values in our core as compared to RC11-120, once again can be attributed to the lack of younger Holocene section in our core.

Another possible cause for this difference might be dissolution, as it affects foraminiferal Mg/Ca ratio (McCorkle et al., 1995; Brown and Elderfield, 1996; Rosenthal et al., 2000; Regenberg et al., 2006). It is possible that *G. bulloides* Mg/Ca at the core site is affected by partial dissolution as the core site lies below the modern carbonate saturation horizon. However, based on multinet and core-top samples, Friedrich et al. (2012) concluded that dissolution does not affect Mg/Ca of *G. bulloides*. Mekik et al. (2007) also suggested that *G. bulloides* Mg/Ca is mainly controlled by calcification temperature and is not susceptible to carbonate dissolution. Brown and Elderfield (1996) also suggested that the effect of dissolution on Mg/Ca is species specific, depending on test wall structure and the fact that it may not always alter the original Mg/Ca ratio. Contrary to these findings, Regenberg et al. (2006) reported a marked decrease in Mg/Ca ratio below the carbonate saturation horizon in several planktic foraminifera. A dissolution-related bias in Mg/Ca *G. bulloides* can be assessed by comparing it with change in shell weight. The weight of individual *G. bulloides* shells varies from 12 μg during the early part of MIS 5 to 24 μg during MIS 2. The shell weight increases throughout MIS 4 through MIS 3. This trend in *G. bulloides* shell weight does not correspond with its Mg/Ca, which has no significant variation during this interval. Even at a later interval (~ 15 kyr until core top), while the shell weight decreases, the Mg/Ca increases. Non-corresponding variation in *G. bulloides* shell weight and its Mg/Ca ratio suggest that changes in Mg/Ca at our core site are possibly not hugely affected by dissolution. The non-correspondence between shell weight and Mg/Ca, however, is not a robust indicator of a well-preserved Mg/Ca signal. The shell weight may not well represent dissolution, as the initial shell weight is controlled by various parameters, including optimal growth rate (de Villiers, 2004), and seawater carbonate ion concentration (Barker and Elderfield, 2002). A better approach should be like the one followed by Rosenthal and Lohman (2002), wherein they assessed the effect of dissolution on Mg/Ca

of *Globigerinoides ruber* and *G. sacculifer* by introducing a correction factor based on the shell weight. The development of such a correction factor for *G. bulloides*, however is beyond the scope of this work.

6.2 Productivity changes: Southern Ocean as atmospheric CO₂ regulator

As compared to the early Holocene, the relative abundance of *G. bulloides* is high throughout the last glacial period, especially during MIS 4 and 2. A synchronous increase in fraction $> 63 \mu\text{m}$ is also noted during the MIS 4 as well as the early part of MIS 2. A minor northward shift in hydrographic regime in this region will affect faunal abundance, as *G. bulloides* comprise the major component of subpolar assemblage, which dominates between 40 and 53° S latitudes (Howard and Prell, 1984). Further, the *G. bulloides* abundance increases during austral spring season, suggesting factors such as shallow mixed layer depth and nutrient availability, other than temperature as controls on its distribution (Fairbanks et al., 1982; Thunell and Reynolds, 1984; Reynolds and Thunell, 1985; Sautter and Thunell, 1989, 1991; Ortiz et al., 1995; Mortyn and Charles, 2003; King and Howard, 2003, 2005). The increase in *G. bulloides* relative abundance and fraction $> 63 \mu\text{m}$ suggests high productivity in the southwestern Indian Ocean during cold periods. The high productivity during cold periods as inferred from *G. bulloides* relative abundance is further supported by increased abundance of *N. incompta*. The lag between *N. incompta* and *G. bulloides* peak in abundance during both MIS 4 and MIS 2 is, however, noted and is attributed to the difference in timing of advection of southern source water, turbulent mixing in the ARR and productivity, and is discussed in the next section. Several studies have suggested increased productivity in the region north of subantarctic zone of the Southern Ocean during the glacial period (Sigman and Boyle, 2000; Jaccard et al., 2013). The high productivity in this region is likely related to the enhanced availability of nutrients as a result of strengthening and equatorward shift of westerlies, as suggested by Toggweiler et al. (2006), based on modeling studies. The strengthening of Southern Hemisphere westerlies between 36 and 43° S during the glacial period, as compared to interglacial, was also inferred by Shulmeister et al. (2004) based on a synthesis of a large number of paleodata. The exact nature of Southern Hemisphere westerlies during glacial periods, however, is debated (Chavaillaz et al., 2013; Sime et al., 2013).

6.3 Difference in *G. bulloides* and *N. incompta* abundance: water column structure, strengthened westerlies, southern source water and migrating STF

The unique feature of our record is an abrupt increase in *G. bulloides* relative abundance during MIS 4 and the later

part of MIS 2, with a synchronous increase in planktic foraminiferal number and fraction $> 63 \mu\text{m}$ during MIS 4, suggesting high-productivity events. A change in *G. bulloides* and planktic foraminiferal abundance, along with variation in coarse fraction percentage in SWIOC, can be interpreted as migration of a high-productivity belt centered at the southern boundary of the STF and the northern boundary of the SAF. We therefore suggest that increased interaction of warm and salty ARC water with the cold SAF waters over the core site (due to northward migration of the STF) might have led to increased productivity observed as increased abundance of *G. bulloides*. Increased abundance of *G. bulloides* has been suggested as an indicator of more austral spring season-like conditions (King and Howard, 2003). It would lead to more intense ARC, as model simulations suggest that the circulation in the Agulhas Recirculation Region strengthens during austral spring through summer in response to intense winds (Matano et al., 1999). Previously, increased productivity and low seawater temperatures during each glacial period were interpreted as northward migration of the subtropical front, further closing the Agulhas Current (Bard and Rickaby, 2009).

The later part of both of these high *G. bulloides* relative abundance events, however, also coincides with an increase in abundance of *N. incompta*. The peak abundance of *N. incompta* is strongly associated with both the pycnocline depth in the Southern Ocean, which is most likely controlled by the thermocline, as well as productivity (Mortyn and Charles, 2003). The *N. incompta* peak flux in this region is observed during austral summer (King and Howard, 2005). The *N. incompta* abundance is comparatively high in the region off the southern tip of Africa as well as the southeastern Atlantic Ocean, as compared with the ARR (Žarić et al., 2006). The variations in abundance of *N. incompta* can thus be linked either to an overall strengthening of ARC, as it can bring more southern-sourced water to the ARR or increased seasonality. Thus the peak *N. incompta* abundance suggests that a part of the high-productivity events in the southwestern Indian Ocean during cold periods is associated with strong seasonality and warming. The beginning of significant increase in the abundance of *G. bulloides* prior to *N. incompta* thus suggests that the northward migration of the STF preceded and probably forced strengthening of the ARC. The increased abundance of *N. incompta* only in the later part of MIS 4 and 2 suggests that a critical point was reached during this time, when either the strengthened westerlies or equatorward shift in the STF forced strong seasonality and advection of southern-sourced water into the ARR, resulting in increased abundance of both *G. bulloides* and *N. incompta* (Simon et al., 2013). The average position of the Subantarctic Front at the LGM (LGM–SAF) was at 43°S (Brathauer and Abelmann, 1999; Gersonde et al., 2003, 2005). This work further suggests that during the LGM the position of STF was more northerly than that off the southern tip of Africa, where it was same as that at present (Gersonde et al., 2003). Earlier,

Bé and Duplessy (1976) suggested that the northern limit of STF in the southwestern Indian Ocean during the glacial period was up to 31°S . These findings were further confirmed by Bard and Rickaby (2009), who reported the migration of the STF to as far north as $\sim 33^\circ \text{S}$ in this region based on faunal and sediment characteristics in core MD962077, which was collected from the southwestern Indian Ocean.

A part of the increase in *N. incompta* was also accompanied by a corresponding increase in *G. bulloides* Mg/Ca, suggesting the warming of the entire water column. The concurrent increase in relative abundance of both *G. bulloides* and *N. incompta*, further suggests strong thermocline. It implies that the upwelling-induced the supply of nutrients to support the high-productivity events (as inferred from *G. bulloides* relative abundance) was seasonal in nature, as the year-long upwelling would have dissipated the thermocline, which should result in decreased *N. incompta* relative abundance. Thus we infer that seasonal high productivity and strong thermocline prevailed during glacial period. The increased abundance of both *G. bulloides* and *N. incompta* was most likely driven by the strong Southern Hemisphere westerlies, as the strong winds during the glacial period will result in a deeper mixed layer and increased nutrient availability, which is reflected in high *N. incompta* relative abundance. This evidence that warming was more pronounced in and most likely confined to the subsurface waters, confirms the model studies which find that the non-breaking surface wave-induced mixing in the Southern Ocean can reduce sea surface temperature and increase subsurface temperature of the upper ocean (Huang et al., 2012).

A peculiar feature of our record is MIS 3 for which the abundance of *N. incompta*, planktic foraminifera and fraction $> 63 \mu\text{m}$ is consistently high, whereas the abundance of *G. bulloides* decreases along with a concurrent decrease in Mg/Ca temperature. The consistently high *N. incompta* abundance during MIS 3 is attributed to enhanced cross-frontal mixing of southern-sourced waters into the ARR due to increased transport in the Agulhas Return Current as a result of increase in turbulence associated with strengthened Southern Hemisphere westerlies (Simon et al., 2013). The strengthened Southern Hemisphere westerlies increased cross-frontal mixing by weakening the thermal gradients associated with the STF. The cross-frontal mixing leads not only to increased export of Indian Ocean waters to the south, leading to decreased *G. bulloides* abundance, but also entrainment of Southern Ocean-derived water masses into the Agulhas Return Current, resulting in increased abundance of *N. incompta* (Simon et al., 2013). Recently, Sime et al. (2013) suggested that a few degrees' equatorward shift of the Southern Hemisphere westerlies during the LGM was likely based on their atmospheric modeling study.

It should, however, be kept in mind that the changes in Agulhas leakage, which in turn affect ARC, are controlled not only by the position of STF but also by the wind strength, position and inertia (Beal et al., 2011). The Agulhas leakage

will increase due to reduced inertia if the wind strength decreases without an accompanying latitudinal shift, and vice-versa. The combined effect of equatorward or poleward shift of wind regime, accompanied by a change in wind strength is thus not clear.

6.4 Subtle temperature salinity change: role of Agulhas retroreflection current

The LGM–early Holocene Mg/Ca temperature difference in the southwestern Indian Ocean is only 1.2 ± 1.2 °C, which is lower than that in the southeastern Indian Ocean (3.5 ± 0.4 °C) (Mashiotta et al., 1999) (Fig. 4). The error here is calculated from the standard deviation of the average Mg/Ca temperature during the Holocene and LGM. This LGM–early Holocene SST difference is also lower than radiolarian-based estimates, which suggest that LGM summer sea surface temperature around the core site was ~ 4 – 5 °C cooler as compared to modern SST (Gersonde et al., 2005). This difference between seawater temperature based on radiolarian transfer function and foraminiferal Mg/Ca may, however, be due to distinct seasonality in abundance of radiolarian and foraminifera. It should be further noted here that this small difference in temperature may partly reflect lack of a complete Holocene section in SWIOC. The difference in LGM–early Holocene $\delta^{18}\text{O}$ *G. bulloides* (1.45 ± 0.6 ‰) in the southwestern Indian Ocean is, however larger than that in the southeastern Indian Ocean (1.23 ± 0.4 ‰). Considering average ice-volume contribution of 1.0 ± 0.1 % over the glacial–interglacial transition (Schrag et al., 2002) leaves 0.45 ± 0.6 ‰ $\delta^{18}\text{O}$, which includes both temperature and salinity components.

Removing the temperature component (0.2 ‰ change per 1 °C change in temperature) results in 0.2 ‰ $\delta^{18}\text{O}$, which can be attributed to local salinity changes (Duplessy et al., 1991). We suggest that comparatively less cooling in the southwestern Indian Ocean during the last glacial period is due to the enhanced influence of the ARC. Increased transport of subtropical warm water by the ARC will warm the Agulhas Recirculation Region. Previous studies have also suggested that the transport of warm and salty water from the Indian to South Atlantic Ocean continued throughout the LGM, but with reduced intensity (Gersonde et al., 2003). The reduced Agulhas leakage was probably driven by increased wind stress in this region. Large wind stress amplitude can trigger turbulent regime, which decreases the availability of Indian Ocean water for the Agulhas leakage (Matano, 1996; Matano et al., 1999; Le Bars et al., 2012; Simon et al., 2013). Recently it was reported that high wind stress in the southwestern Indian Ocean decreases the rate or cessation of eddy shedding by the AC, leading to increased retroreflection and delayed transport of previously shed eddy further westward into the Atlantic Ocean and thus increases seawater temperature off the southern tip of Africa (van Aken et al., 2013). Increased influence of ARC (relatively warm and stratified

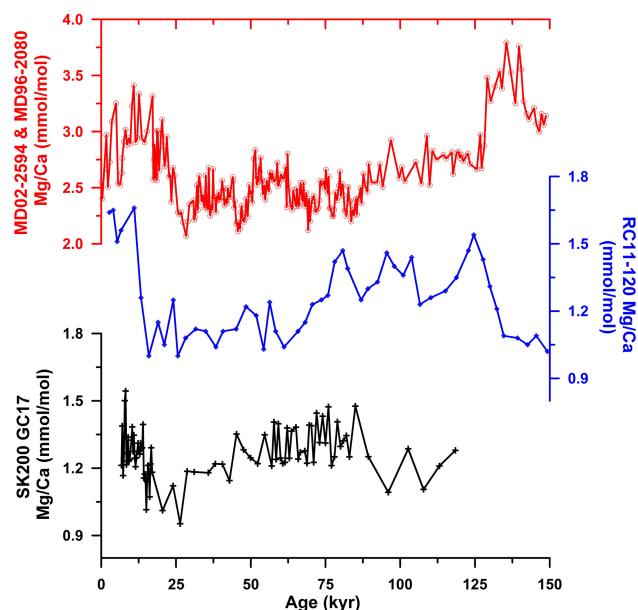


Fig. 4. A comparison of *Globigerina bulloides* Mg/Ca in core SK 200 GC17 with that in RC11-120 which was collected from southeastern Indian Ocean (Mashiotta et al., 1999) and MD02-2594 and MD96-2080 (Martínez-Méndez et al., 2010). The Mg/Ca scale (y axis) is the same for SK 200 GC17 and RC11-120.

surface waters) off the southern tip of Africa, a region which lies in the path of Agulhas Current and eddy shedding, during MIS 1 and 5 and decreased influence during MIS 2 and 4, was also inferred from changes in coccolithophores (Flores et al., 1999). Peeters et al. (2004) also inferred enhanced Indian–Atlantic water exchange during the present and last interglacial, with reduced exchange during the glacial periods. The region west of the southern tip of Africa will show signatures of AC, while the region east of it is influenced by the ARC, thus recording opposite signals.

The Mg/Ca SST during the last glacial period prior to the LGM was comparable with the early Holocene SST. Though the sample resolution is coarse, a progressive increase in sea surface temperature during the glacial period is also noticed, as previously reported from the southwestern Indian Ocean (Martínez-Méndez et al., 2010) (Fig. 4). The beginning of glacial warming during the MIS 2 coincides with the warming reported from the region further west of SWIOC (Martínez-Méndez et al., 2010). We are, however, unable to comment on the extent of this warming relative to the late Holocene, as the later section is missing in SWIOC. The $\delta^{18}\text{O}$ *G. bulloides* was depleted in the southwestern Indian Ocean as compared with the southeastern Indian Ocean throughout the last glacial period (Fig. 5). The difference was more pronounced during MIS 3. During the last glacial period, the difference in seawater temperature as estimated from *G. bulloides* Mg/Ca, however, was smaller than that at present (6.5 °C). Additionally during MIS 2, the temperature

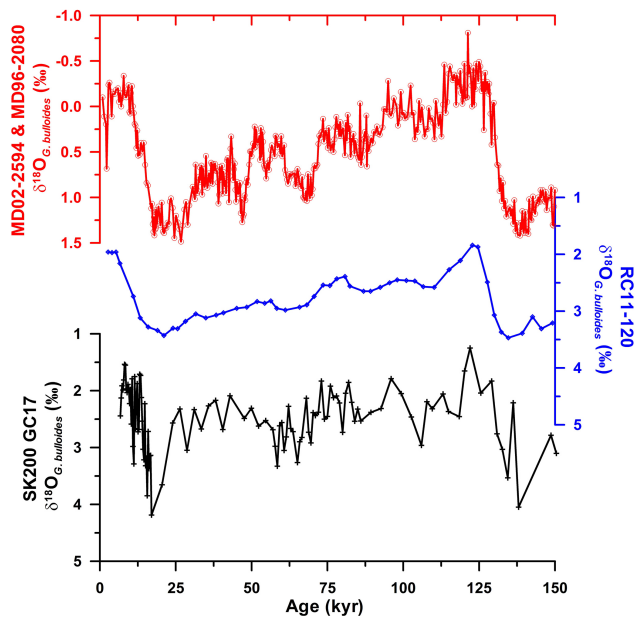


Fig. 5. A comparison of *Globigerina bulloides* $\delta^{18}\text{O}$ in core SK 200 GC17 with that in RC11-120, which was collected from southeastern Indian Ocean ($43^{\circ}31'\text{S}$, $79^{\circ}52'\text{E}$; 3135 m water depth; Mashiotta et al., 1999) and MD02-2594 and MD96-2080 (MD02-2594: $33^{\circ}18'\text{S}$, $17^{\circ}18'\text{E}$; 2440 m water depth; MD96-2080: $36^{\circ}16'\text{S}$, $19^{\circ}28'\text{E}$; 2488 m water depth; Martínez-Méndez et al., 2010). The actual *G. bulloides* $\delta^{18}\text{O}$ values of core SK 200/17 are plotted, without taking the running average. The $\delta^{18}\text{O}$ scale (y axis) is the same for SK 200 GC17 and RC11-120.

of both of these regions was the same. It further supports our hypothesis of strengthening of the Agulhas Return Current, resulting in a supply of warm water to the Indian sector of the Southern Ocean. The strengthened ARC warmed the entire Indian sector of the Southern Ocean, thus resulting in decreased longitudinal seawater temperature gradient. Therefore, we attribute the unique nature of our record to changes in the strength and position of the ARC, which drives the hydrology around the core site.

6.5 Changes during termination I

An interesting feature of this record is a drastic decline in *G. bulloides* abundance just prior to the last glacial maximum. The Mg/Ca temperature is also the lowest at this time, while $\delta^{18}\text{O}$ *G. bulloides* is yet to reach its most enriched LGM level. The recovery phase of *G. bulloides* relative abundance during early MIS 2 coincides with an increase in Mg/Ca temperature. The peak *G. bulloides* relative abundance coincides with a peak in *N. incompta* relative abundance. The planktic foraminiferal abundance and fraction $> 63\ \mu\text{m}$, however, is at its lowest during this time. Both planktic foraminiferal abundance and fraction $> 63\ \mu\text{m}$ indicate either low productivity or a poor preservation of foraminiferal tests. The

mid-transition-increased *G. bulloides* abundance indicates increased surface productivity, probably in response to the Antarctic Cold reversal. The decreased *G. bulloides* abundance during late deglaciation indicates decreased surface productivity probably due to meltwater-lid-induced increased stratification (Francois et al., 1993). As high *G. bulloides* relative abundance indicates increased productivity as discussed before, we suggest that the drop in planktic foraminiferal abundance and fraction $> 63\ \mu\text{m}$ during Termination I is the result of poor preservation. The variation in planktic foraminiferal abundance is similar to the change in carbonate percentage (higher during glacial period than during interglacial) observed in cores collected from the southeastern Atlantic off the southwestern coast of Africa (Hodell et al., 2001). A sharp decrease in both the planktic foraminiferal abundance as well as fraction $> 63\ \mu\text{m}$ during termination, indicates sharp decline in carbonate percentage during termination, which is a characteristic of cores collected from this region.

7 Conclusions

Based on the faunal, stable isotopic and trace element analysis of planktic foraminifera in a core collected from the southwestern Indian Ocean in the path of Agulhas Retroflexion Current, we infer that over the last glacial–interglacial cycle, the hydrography of this region was driven by change in the strength of westerlies, as well as migrating subtropical front. The productivity in the southwestern Indian Ocean increased during cold periods, which confirms previous reports. The increased productivity during the glacial period suggests northward migration of the subtropical front. The increased relative abundance of *N. incompta* is inferred as a result of strong thermocline and advection of southern-sourced water into the ARC. The findings confirm previous reports of the Southern Ocean as the storehouse of atmospheric carbon during the glacial period.

Supplementary material related to this article is available online at <http://www.clim-past.net/10/745/2014/cp-10-745-2014-supplement.zip>.

Acknowledgements. Authors are thankful to the Director of the National Institute of Oceanography and National Center for Antarctic and Ocean Research for providing the facility to carry out the work. We express our sincere thanks to Rahul Mohan, Program Director, Antarctic Science, of NCAOR, Goa for providing all the support for this work. V. K. Banakar and Anita Garg of NIO, Goa are thankfully acknowledged for the stable oxygen isotopic measurements. The help of David Lea and Georges Paradis of the University of California, Santa Barbara in analyzing the trace element ratio is sincerely acknowledged. We are thankful to the two anonymous reviewers and M. H. Simon for the suggestions which

helped to improve the manuscript. This work is a part of the project funded by NCAOR Goa, India. The help of Sujata Kurtarkar in picking foraminiferal specimens is thankfully acknowledged.

Edited by: A. Elmore

References

- Anilkumar, N., Luis, A. J., Somayajulu, Y. K., Ramesh Babu, V. M., Dash, K., Pednekar, S. M., Babu, K. N., Sudhakar, M., and Pandey, P. C.: Fronts, water masses and heat content variability in the Western Indian sector of the Southern Ocean during austral summer 2004, *J. Mar. Syst.*, 63, 20–34, 2006.
- Antonov, J. I., Seidov, D., Boyer, T. P., Locarnini, R. A., Mishonov, A. V., Garcia, H. E., Baranova, O. K., Zweng, M. M., and Johnson, D. R.: World Ocean Atlas 2009, in: Volume 2: Salinity, edited by: Levitus, S., NOAA Atlas NESDIS 69, US Government Printing Office, Washington, D.C., 184 pp., 2010.
- Bader, J. and Latif, M.: The impact of decadal-scale Indian Ocean sea surface temperature anomalies on Sahelian rainfall and the North Atlantic Oscillation, *Geophys. Res. Lett.*, 30, 2169, doi:10.1029/2003GL018426, 2003.
- Bard, E. and Rickaby, R. E. M.: Migration of the subtropical front as a modulator of glacial climate, *Nature*, 460, 380–383, 2009.
- Barker, S. and Elderfield, H.: Foraminiferal calcification response to glacial-interglacial changes in atmospheric CO₂, *Science*, 297, 833–836, 2002.
- Barker, S., Cacho, I., Benway, H., and Tachikawa, K.: Planktonic foraminiferal Mg/Ca as a proxy for past oceanic temperatures: a methodological overview and data compilation for the Last Glacial Maximum, *Quaternary Sci. Rev.*, 24, 821–834, 2005.
- Barker, S., Diz, P., Vautravers, M. J., Pike, J., Knorr, G., Hall, I. R., and Broecker, W. S.: Interhemispheric Atlantic seesaw response during the last deglaciation, *Nature*, 457, 1097–1102, 2009.
- Bassinot, F. C., Labeyrie, L. D., Vincent, E. X. Q., Shackleton, N. J., and Lancelot, Y.: The astronomical theory of climate and the age of the Brunhes-Matuyama magnetic reversal, *Earth Planet. Sc. Lett.*, 126, 91–108, 1994.
- Bé, A. W. H. and Duplessy, J. C.: Subtropical convergence fluctuations and quaternary climates in the middle latitudes of the Indian Ocean, *Science*, 194, 419–422, 1976.
- Bé, A. W. H. and Hutson, W. H.: Ecology of planktonic foraminifera and biogeographic patterns of life and fossil assemblages in the Indian Ocean, *Micropaleontology*, 23, 369–414, 1977.
- Beal, L. M., De Ruijter, W. P. M., Biastoch, A., Zahn, R., and SCOR/WCRP/IAPSO Working Group: On the role of the Agulhas system in ocean circulation and climate, *Nature*, 472, 429–436, 2011.
- Bergami, C., Capotondi, L., Langone, L., Giglio, F., and Ravaioli, M.: Distribution of living planktonic foraminifera in the Ross Sea and the Pacific sector of the Southern Ocean (Antarctica), *Mar. Micropaleontol.*, 73, 37–48, 2009.
- Berger, W. H.: Deep-Sea carbonates: dissolution profiles from foraminiferal preservation, Cushman Foundation for Foraminiferal Research Special Publication, 13, 82–86, 1975.
- Brathauer, U. and Abelmann, A.: Late Quaternary variations in sea surface temperatures and their relationship to orbital forcing recorded in the Southern Ocean (Atlantic sector), *Paleoceanography*, 14, 135–148, 1999.
- Brown, S. J. and Elderfield, H.: Variations in Mg/Ca and Sr/Ca ratios of planktonic foraminifera caused by postdepositional dissolution: evidence of a shallow Mg-dependent dissolution, *Paleoceanography*, 11, 543–551, 1996.
- Bryden, H. L. and Beal, L. M.: Role of the Agulhas Current in Indian Ocean circulation and associated heat and freshwater fluxes, *Deep-Sea Res. Pt. I*, 48, 1821–1845, 2001.
- Caley, T., Giraudeau, J., Malaizé, B., Rossignol, L., and Pierre, C.: Agulhas leakage as a key process in the modes of Quaternary climate changes, *P. Natl. Acad. Sci.*, 109, 6835–6839, doi:10.1073/pnas.1115545109, 2012.
- Chavaillaz, Y., Codron, F., and Kageyama, M.: Southern westerlies in LGM and future (RCP4.5) climates, *Clim. Past*, 9, 517–524, doi:10.5194/cp-9-517-2013, 2013.
- Chave, K. E.: Aspects of the biogeochemistry of magnesium I. Calcareous marine organisms, *J. Geol.*, 62, 266–283, 1954.
- Clemens, S. C., Prell, W. L., Murray, D., Shimmield, G., and Weedon, G.: Forcing mechanisms of the Indian Ocean monsoon, *Nature*, 353, 720–725, 1991.
- Darling, K. F., Kucera, M., Kroon, D., and Wade, C. M.: A resolution for the coiling direction paradox in *Neoglobobadrina pachyderma*, *Paleoceanography*, 21, PA2011, doi:10.1029/2005PA001189, 2006.
- De Boer, A. M., Graham, R. M., Thomas, M. D., and Kohfeld, K. E.: The control of the Southern Hemisphere Westerlies on the position of the Subtropical Front, *J. Geophys. Res.-Oceans*, 118, 5669–5675, doi:10.1002/jgrc.20407, 2013.
- de Ruijter, W. P. M., Biastoch, A., Drijfhout, S. S., Lutjeharms, J. R. E., Matano, R. P., Pichevin, T., van Leeuwen, P. J., and Weijer, W.: Indian-Atlantic interocean exchange: dynamics, estimation and impact, *J. Geophys. Res.*, 104, 20885–20910, 1999.
- de Ruijter, W. P. M., Ridderinkhof, H., and Schouten, M. W.: Variability of the southwest Indian Ocean, *Philos. T. Roy. Soc. A*, 363, 63–76, 2005.
- de Villiers, S.: Optimum growth conditions as opposed to calcite saturation as a control on the calcification rate and shell-weight of marine foraminifera, *Mar. Biol.*, 144, 45–49, 2004.
- Donohue, K. A. and Toole, J.: A near-synoptic survey of the Southwest Indian Ocean, *Deep-Sea Res.*, 50, 1893–1931, 2003.
- Duplessy, J. C., Labeyrie, L., Juillet-Leclerc, A., Maitre, F., Duprat, J., and Sarnthein, M.: Surface salinity reconstruction of the north Atlantic Ocean during the last glacial maximum, *Oceanol. Acta*, 14, 311–324, 1991.
- Durgadoo, J. V., Loveday, B. R., Reason, C. J. C., Penven, P., and Biastoch, A.: Agulhas leakage predominantly responds to the Southern Hemisphere westerlies, *J. Phys. Oceanogr.*, 43, 2113–2131, doi:10.1175/JPO-D-13-047.1, 2013.
- Ericson, D. B.: Coiling direction of *Globigerina pachyderma* as a climatic index, *Science*, 130, 219–220, 1959.
- Fairbanks, R. G., Sverdrlove, M. S., Free, R., Wiebe, P. H., and Bé, A. W. H.: Vertical distribution and isotopic fractionation of living planktonic foraminifera from the Panama Basin, *Nature*, 298, 841–844, 1982.
- Fine, R. A.: Direct evidence using tritium data for throughflow from the Pacific into the Indian Ocean, *Nature*, 315, 478–480, 1985.
- Flores, J. A., Gersonde, R., and Sierro, F. J.: Pleistocene fluctuations in the Agulhas Current Retroflexion based on the calcareous plankton record, *Mar. Micropaleontol.*, 37, 1–22, 1999.

- Fraile, I., Schulz, M., Mulitza, S., and Kucera, M.: Predicting the global distribution of planktonic foraminifera using a dynamic ecosystem model, *Biogeosciences*, 5, 891–911, doi:10.5194/bg-5-891-2008, 2008.
- Fraile, I., Schulz, M., Mulitza, S., Merkel, U., Prange, M., and Paul, A.: Modeling the seasonal distribution of planktonic foraminifera during the Last Glacial Maximum, *Paleoceanography*, 24, PA2216, doi:10.1029/2008PA001686, 2009.
- Francois, R., Bacon, M. P., Altabet, M. A., and Labeyrie, L. D.: Glacial/interglacial changes in sediment rain rate in the SW Indian Sector of subantarctic Waters as recorded by ^{230}Th , ^{231}Pa , U, and $\delta^{15}\text{N}$, *Paleoceanography*, 8, 611–629, doi:10.1029/93PA00784, 1993.
- Friedrich, O., Schiebel, R., Wilson, P. A., Weldeab, S., Beer, C. J., Cooper, M. J., and Fiebig, J.: Influence of test size, water depth, and ecology on Mg/Ca, Sr/Ca, $\delta^{18}\text{O}$ and ^{13}C in nine modern species of planktic foraminifers, *Earth Planet. Sc. Lett.*, 319–320, 133–145, 2012.
- Gersonde, R., Abelmann, A., Brathauer, U., Becquey, S., Bianchi, C., Cortese, G., Grobe, H., Kuhn, G., Niebler, H. S., Segl, M., Sieger, R., Zielinski, U., and Fütterer, D. K.: Last glacial sea surface temperatures and sea-ice extent in the Southern Ocean (Atlantic-Indian sector): A multiproxy approach, *Paleoceanography*, 18, 6-1–6-18, 2003.
- Gersonde, R., Crosta, X., Abelmann, A., and Armand, L.: Sea-surface temperature and sea ice distribution of the Southern Ocean at the epilog Last Glacial Maximum—A circum-Antarctic view based on siliceous microfossil records, *Quaternary Sci. Rev.*, 24, 869–896, 2005.
- Gordon, A. L.: Interocean exchange of thermocline water, *J. Geophys. Res.*, 91, 5037–5046, 1986.
- Graham, R. M. and De Boer, A. M.: The Dynamical Sub-tropical Front, *J. Geophys. Res.-Oceans*, 118, 5676–5685, doi:10.1002/jgrc.20408, 2013.
- Gupta, A. K., Anderson, D. M., and Overpeck, J. T.: Abrupt changes in the Asian southwest monsoon during the Holocene and their links to the North Atlantic Ocean, *Nature*, 421, 354–357, 2003.
- Hemleben, Ch., Spindler, M., and Anderson, O. R.: *Modern Planktonic Foraminifera*, 1st Edn., Springer-Verlag Inc., New York, 363 pp., 1989.
- Hodell, D. A., Charles, C. D., and Sierro, F. J.: Late Pleistocene evolution of the ocean's carbonate system, *Earth Planet. Sc. Lett.*, 192, 109–124, 2001.
- Howard, W. R. and Prell, W. L. A.: Comparison of Radiolarian and Foraminiferal Paleocology in the Southern Indian Ocean: New Evidence for the Interhemispheric Timing of Climatic Change, *Quaternary Res.*, 21, 244–263, 1984.
- Howard, W. R. and Prell, W. L.: Late Quaternary CaCO_3 production and preservation in the Southern Ocean: Implications for oceanic and atmospheric carbon cycling, *Paleoceanography*, 9, 453–482, doi:10.1029/93PA03524, 1994.
- Huang, C. J., Qiao, F., Shu, Q., and Song, Z.: Evaluating austral summer mixed-layer response to surface wave-induced mixing in the Southern Ocean, *J. Geophys. Res.*, 117, C00J18, doi:10.1029/2012JC007892, 2012.
- Ito, T., Parekh, P., Dutkiewicz, S., and Follows, M. J.: The Antarctic Circumpolar Productivity Belt, *Geophys. Res. Lett.*, 32, L13604, doi:10.1029/2005GL023021, 2005.
- Jaccard, S. L., Hayes, C. T., Martínez-García, A., Hodell, D. A., Anderson, R. F., Sigman, D. M., and Haug, G. H.: Two modes of change in Southern Ocean productivity over the past million years, *Science*, 339, 1419–1423, 2013.
- Katz, A.: The interaction of magnesium with calcite during crystal growth at 25–90 °C and one atmosphere, *Geochim. Cosmochim. Acta*, 37, 1563–1586, 1973.
- King, A. L. and Howard, W. R.: Planktonic foraminiferal flux seasonality in Subantarctic sediment traps: A test for paleoclimate reconstructions, *Paleoceanography*, 18, 19-1–19-17, 2003.
- King, A. L. and Howard, W. R.: $\delta^{18}\text{O}$ seasonality of planktonic foraminifera from the Southern Ocean sediment traps: Latitudinal gradients and implications for paleoclimate reconstructions, *Mar. Micropal.*, 56, 1–24, 2005.
- Knorr, G. and Lohmann, G.: Southern Ocean origin for the resumption of Atlantic thermohaline circulation during deglaciation, *Nature*, 424, 532–536, 2003.
- Kohfeld, K. E., Graham, R. M., d. Boer, A. M., Sime, L. C., Wolff, E. W., Quéré, C. L., and Bopp, L.: Southern Hemisphere westerly wind changes during the Last Glacial Maximum: Paleo-data synthesis, *Quaternary Sci. Rev.*, 64, 104–120, 2013.
- Kuroyangi, A. and Kawahata, H.: Vertical distribution of living planktonic foraminifera in the seas around Japan, *Mar. Micropaleontol.*, 53, 173–196, 2004.
- Lea, D. W., Mashiotto, T. A., and Spero, H. J.: Controls on magnesium and strontium uptake in planktonic foraminifera determined by live culturing, *Geochim. Cosmochim. Acta*, 63, 2369–2379, 1999.
- Le Bars, D., De Ruijter, W. P. M., and Dijkstra, H. A.: A New Regime of the Agulhas Current Retroflexion: Turbulent Choking of Indian-Atlantic leakage, *J. Phys. Oceanogr.*, 42, 1158–1172, 2012.
- Lisiecki, L. E. and Raymo, M. E.: A Pliocene-Pleistocene stack of 57 globally distributed benthic $\delta^{18}\text{O}$ records, *Paleoceanography*, 20, PA1003, doi:10.1029/2004PA001071, 2005.
- Locarnini, R. A., Mishonov, A. V., Antonov, J. I., Boyer, T. P., Garcia, H. E., Baranova, O. K., Zweng, M. M., and Johnson, D. R.: *World Ocean Atlas 2009*, in: Volume 1: Temperature, edited by: Levitus, S., NOAA Atlas NESDIS 68, US Government Printing Office, Washington, D.C., 184 pp., 2010.
- Lutjeharms, J. R. E. and Ansorge, I. J.: The Agulhas Return Current, *J. Mar. Syst.*, 30, 115–138, 2001.
- Lutjeharms, J. R. E. and van Ballegooyen, R. C.: The retroflexion of the Agulhas Current, *J. Phys. Oceanogr.*, 18, 1570–1583, 1988.
- Marino, G., Zahn, R., Ziegler, M., Purcell, C., Knorr, G., Hall, I. R., Ziveri, P., and Elderfield, H.: Agulhas salt-leakage oscillations during abrupt climate changes of the Late Pleistocene, *Paleoceanography*, 28, 599–606, 2013.
- Martin, P. A. and Lea, D. W.: A simple evaluation of cleaning procedures on fossil benthic foraminiferal Mg/Ca, *Geochem. Geophys. Geosy.*, 3, 1–8, 2002.
- Martínez-Méndez, G., Zahn, R., Hall, I. R., Peeters, F. J. C., Pena, L. D., Cacho, I., and Negre, C.: Contrasting multiproxy reconstructions of surface ocean hydrography in the Agulhas Corridor and implications for the Agulhas Leakage during the last 345,000 years, *Paleoceanography*, 25, PA4227, doi:10.1029/2009PA001879, 2010.

- Mashiotta, T. A., Lea, D. W., and Spero, H. J.: Glacial–interglacial changes in Subantarctic sea surface temperature and $\delta^{18}\text{O}$ -water using foraminiferal Mg, *Earth Planet. Sc. Lett.*, 170, 417–432, 1999.
- Matano, R. P.: A numerical study of the Agulhas retroflexion: The role of bottom topography, *J. Phys. Oceanogr.*, 26, 2267–2278, 1996.
- Matano, R. P., Simionato, C. G., de Ruijter, W. P., van Leeuwen, P. J., Strub, P. T., Chelton, D. B., and Schlax, M. G.: Seasonal variability in the Agulhas Retroflexion region, *Geophys. Res. Lett.*, 25, 4361–4364, 1998.
- Matano, R. P., Simionato, C. G., and Strub, P. T.: Modeling the wind-driven variability of the south Indian Ocean, *J. Phys. Oceanogr.*, 29, 217–230, 1999.
- McCorkle, D. C., Martin, P. A., Lea, D. W., and Klinkhammer, G. P.: Evidence of a dissolution effect on benthic foraminiferal shell chemistry: $\delta^{13}\text{C}$, Cd/Ca, Ba/Ca and Sr/Ca from the Ontong Java Plateau, *Paleoceanography*, 10, 699–714, 1995.
- McCreary, J. P., Kohler Jr., K. E., Hood, R. R., and Olson, D. B.: A four-component ecosystem model of biological activity in the Arabian Sea, *Prog. Oceanogr.*, 37, 193–240, 1996.
- Mekik, F., Francois, R., and Soon, M.: A novel approach to dissolution correction of Mg/Ca-based paleothermometry in the tropical Pacific, *Paleoceanography*, 22, PA3217, doi:10.1029/2007PA001504, 2007.
- Mortyn, P. G. and Charles, C. D.: Planktonic foraminiferal depth habitat and $\delta^{18}\text{O}$ calibrations: Plankton tow results from the Atlantic sector of the Southern Ocean, *Paleoceanography*, 18, 15–1–15–14, doi:10.1029/2001PA000637, 2003.
- Oomori, T., Kaneshima, H., and Maezato, Y.: Distribution coefficient of Mg^{2+} ions between calcite and solution at 10–50 °C, *Mar. Chem.*, 20, 327–336, 1987.
- Ortiz, J. D., Mix, A. C., and Collier, R. W.: Environmental control of living symbiotic and asymbiotic foraminifera of the California Current, *Paleoceanography*, 10, 987–1009, 1995.
- Peeters, F. J. C., Brummer, G. J. A., and Ganssen, G. M.: The effect of upwelling on the distribution and stable isotope composition of *Globigerina bulloides* and *Globigerinoides ruber* (planktic foraminifera) in modern surface waters of the NW Arabian Sea, *Global Planet. Change*, 34, 269–291, 2002.
- Peeters, F. J. C., Acheson, R., Brummer, G. J. A., de Ruijter, W. P. M., Schneider, R. R., Ganssen, G. M., Ufkes, E., and Kroon, D.: Vigorous exchange between the Indian and Atlantic oceans at the end of the past five glacial periods, *Nature*, 430, 661–665, 2004.
- Poulton, A. J., Stinchcombe, M. C., and Quartly, G. D.: High numbers of *Trichodesmium* and diazotrophic diatoms in the southwest Indian Ocean, *Geophys. Res. Lett.*, 36, L15610, doi:10.1029/2009GL039719, 2009.
- Prell, W. L. and Curry, W. B.: Faunal and isotopic indices of monsoonal upwelling: western Arabian Sea, *Oceanol. Acta.*, 4, 91–98, 1981.
- Quartly, G. D. and Srokosz, M. A.: Seasonal variations in the region of the Agulhas Retroflexion: Studies with Geosat and FRAM, *J. Phys. Oceanogr.*, 23, 2107–2124, 1993.
- Quartly, G. D., Buck, J. J. H., Srokosz, M. A., and Coward, A. C.: Eddies around Madagascar: The retroflexion re-considered, *J. Mar. Syst.*, 63, 115–129, 2006.
- Rau, A. J., Rogers, J., Lutjeharms, J. R. E., Giraudeau, J., Lee-Thorp, J. A., Chen, M. T., and Waelbroeck, C.: A 450-kyr record of hydrological conditions on the western Agulhas Bank slope, south of Africa, *Mar. Geol.*, 180, 183–201, 2002.
- Read, J. F. and Pollard, R. T.: Structure and transport of Antarctic circumpolar current and Agulhas Return Current at 40° E, *J. Geophys. Res.*, 98, 12281–12295, 1993.
- Regenberg, M., Nürnberg, D., Steph, S., Groeneveld, J., Garbe-Schönberg, D., Tiedemann, R., and Dullo, W. C.: Assessing the effect of dissolution on planktonic foraminiferal Mg/Ca ratios: Evidence from Caribbean core tops, *Geochem. Geophys. Geosy.*, 7, Q07P15, doi:10.1029/2005GC001019, 2006.
- Reynolds, L. A. and Thunell, R. C.: Seasonal succession of planktonic foraminifera in the subpolar North Pacific, *J. Foramin. Res.*, 15, 282–301, 1985.
- Rintoul, S. R., Hughes, C., and Olbers, D.: The Antarctic Circumpolar Current system, in: *Ocean Circulation and Climate*, edited by: Siedler, J. C. G. and Gould, J., Academic Press, London, 271–302, 2001.
- Rosenthal, Y. and Lohmann, G. P.: Accurate estimation of sea surface temperatures using dissolution-corrected calibrations for Mg/Ca paleothermometry, *Paleoceanography*, 17, 16–1–16–6, doi:10.1029/2001PA000749, 2002.
- Rosenthal, Y., Lohman, G. P., Lohman, K. C., and Sherrell, R. M.: Incorporation and preservation of Mg in *Globigerinoides sacculifer*: Implications for reconstructing the temperature and $^{18}\text{O}/^{16}\text{O}$ of seawater, *Paleoceanography*, 15, 135–145, 2000.
- Sautter, L. R. and Thunell, R. C.: Seasonal succession of planktonic foraminifera: Results from a four-year time-series sediment trap experiment in the northeast Pacific, *J. Foramin. Res.*, 19, 253–267, 1989.
- Sautter, L. R. and Thunell, R. C.: Planktonic foraminiferal response to upwelling and seasonal hydrographic conditions: Sediment trap results from San Pedro Basin, Southern California Bight, *J. Foramin. Res.*, 21, 347–363, 1991.
- Schiebel, R., Bijma, J., and Hemleben, C.: Population dynamics of the planktic foraminifer *Globigerina bulloides* from the eastern North Atlantic, *Deep-Sea Res. Pt. I*, 44, 1701–1713, 1997.
- Schott, F. A., Xie, S. P., and McCreary Jr., J. P.: Indian Ocean circulation and climate variability, *Rev. Geophys.*, 47, RG1002, doi:10.1029/2007RG000245, 2009.
- Schouten, M. W., de Ruijter, W. P. M., van Leeuwen, P. J., and Lutjeharms, J. R. E.: Translation, decay and splitting of Agulhas rings in the south-east Atlantic Ocean, *J. Geophys. Res.*, 105, 21913–21925, 2000.
- Schrag, D. P., Adkins, J. F., McIntyre, K., Alexander, J. L., Hodell, D. A., Charles, C. D., and McManus, J. F.: The oxygen isotopic composition of seawater during the Last Glacial Maximum, *Quaternary Sci. Rev.*, 21, 331–342, 2002.
- Shulmeister, J., Goodwin, I., Renwick, J., Harle, K., Armand, L., McGlone, M. S., Cook, E., Dodson, J., Hesse, P. P., Mayewski, P., and Curran, M.: The Southern Hemisphere westerlies in the Australasian sector over the last glacial cycle: A synthesis, *Quatern. Int.*, 118/119, 23–53, 2004.
- Sigman, D. M. and Boyle, E. A.: Glacial/interglacial variations in atmospheric carbon dioxide, *Nature*, 407, 859–869, 2000.

- Sime, L. C., Kohfeld, K. E., Le Quéré, C., Wolff, E. W., de Boer, A. M., Graham, R. M., and Bopp, L.: Southern Hemisphere westerly wind changes during the Last Glacial Maximum: model-data comparison, *Quaternary Sci. Rev.*, 64, 104–120, 2013.
- Simon, M. H., Arthur, K. L., Hall, I. R., Peeters, F. J. C., Love-day, B. R., Barker, S., Ziegler, M., and Zahn, R.: Millennial-scale Agulhas Current variability and its implications for salt-leakage through the Indian–Atlantic Ocean Gateway, *Earth Planet. Sc. Lett.*, 383, 101–112, 2013.
- Stramma, L.: The South Indian Ocean Current, *J. Phys. Oceanogr.*, 22, 421–430, 1992.
- Stramma, L. and Lutjeharms, J. R. E.: The flow of the subtropical gyre of the South Indian Ocean, *J. Geophys. Res.*, 102, 5513–5530, 1997.
- Talley, L. D.: Closure of the global overturning circulation through the Indian, Pacific, and Southern Oceans: Schematics and transports, *Oceanography* 26, 80–97, doi:10.5670/oceanog.2013.07, 2013.
- Thunell, R. C. and Reynolds, L.: Sedimentation of planktonic foraminifera: Seasonal changes in species flux in the Panama Basin, *Micropaleontology*, 30, 241–260, 1984.
- Toggweiler, J. R., Russell, J. L., and Carson, S. R.: Mid-latitude westerlies, atmospheric CO₂, and climate change during the ice ages, *Paleoceanography*, 21, PA2005, doi:10.1029/2005PA001154, 2006.
- Tomczak, M. and Godfrey, J. S.: *Regional Oceanography: An Introduction*, Pergamon, New York, p. 390, 2003.
- van Aken, H. M., Lutjeharms, J. R. E., Rouault, M., Whittle, C., and de Ruijter, W. P. M.: Observations of an early Agulhas Current Retroflexion event in 2001: a temporary cessation of inter-ocean exchange south of Africa?, *Deep-Sea Res. Pt. I*, 72, 1–8, 2013.
- Wyrtki, K.: *Oceanographic Atlas of the International Indian Ocean Expedition*, National Science Foundation, Washington, D.C., 531 pp., 1971.
- Žarić, S., Schulz, M., and Mulitza, S.: Global prediction of planktic foraminiferal fluxes from hydrographic and productivity data, *Biogeosciences*, 3, 187–207, doi:10.5194/bg-3-187-2006, 2006.